Title

Distinguishing the four genetic causes of Jouberts syndrome-related disorders

Journal

Annals of Neurology, 57(4)

ISSN

0364-5134

Authors

Valente, E M
Marsh, S E
Castori, M
et al.

Publication Date

2005-04-01

Peer reviewed

Mutations in the *CEP290* gene, encoding a centrosomal protein, cause pleiotropic forms of Joubert Syndrome

Enza Maria Valente,[1]* Jennifer L. Silhavy,[2]* Francesco Brancati,[1,3] Giuseppe Barrano,[1,4] Suguna Rani Krishnaswami,[2] Marco Castori,[1,4] Madeline A. Lancaster, [2] Eugen Boltshauser,[5] Loredana Boccone,[6] Lihadh Al-Gazali,[7] Elisa Fazzi,[8] Sabrina Signorini,[8] Carrie M. Louie, [2] Emanuele Bellacchio,[1] the International JSRD Study Group, Enrico Bertini,[9] Bruno Dallapiccola,[1,4] Joseph G. Gleeson.[2]

[1]IRCCS CSS, Mendel Institute, viale Regina Margherita 261, 00198 Rome, Italy, tel. +39 (06) 4416 0503

[2]Laboratory of Neurogenetics, Department of Neurosciences, University of California, San Diego, Leichtag 332, 9500 Gilman Drive, La Jolla, CA 92093-0691, USA, tel. +1 (858) 822 3535

[3]Department of Biological Sciences, G. D'Annunzio University, Via dei Vestini 31, 66013 Chieti, Italy, tel. +39 (0871) 3554137

[4]Department of Experimental Medicine and Pathology, La Sapienza University, viale Regina Elena 324, 00187 Rome, Italy, tel. +39 (06) 4416 0501

[5]Department of Neurology, Children's University Hospital, Steinwiesstrasse 75, 8032 Zurich, Switzerland, tel. +41 (1) 266 7330

[6]Ospedale Microcitemico, Cagliari, Italy, tel. +39 (070) 6095666

[7]Department of Pediatrics, Faculty of Medicine and Health Sciences, United Emirates University, PO Box 17666, Al Ain, United Arab Emirates, tel. +971 (3) 703 9415 and +971 (3) 767 2022

[8]Department of Child Neurology and Psychiatry, IRCCS "C. Mondino Foundation", University of Pavia, Italy, tel. +39 (0382) 380 280

[9]Molecular Medicine Unit, Department of Laboratory Medicine, Bambino Gesu' Hospital IRCCS, Piazza S. Onofrio, 4, 00165 Rome, Italy, tel. +39 (06) 6859 2105

*these two authors contributed equally to this work.

Corresponding author:
Joseph G. Gleeson
University of California-San Diego
Leichtag 332
9500 Gilman Drive
La Jolla, CA 92093-0624

tel. +1 (858) 822 3535
fax. +1 (858) 822 1021
e-mail: jogleeson@ucsd.edu

Introductory paragraph

Joubert syndrome is a severe developmental disorder mainly consisting of ataxia, oculomotor apraxia and mental retardation and characterized by cerebellar vermis hypoplasia and a peculiar brainstem malformation known as the "molar tooth sign"[1,2]. Patients frequently display additional features of cystic kidney disease progressing to renal failure and ocular manifestations including retinopathy, encompassing the Joubert Syndrome Related Disorders (JSRD) group of conditions[3-5]. We used homozygosity mapping to identify a novel locus on chromosome 12 and subsequently truncating mutations in the *centrosomal protein 290* (*CEP290*) gene in four families and a missense mutation in a fifth family. These families display pleiotropic forms of JSRD with variable retinal and renal manifestations. *CEP290* expression was detected in developing murine tissues, most notably in proliferating cerebellar granule neuron populations, and showed centrosome and cilia intracellular localization in non-neuronal cells. Our data imply a direct connection between JSRDs and other cilia/centrosomal human disorders such as isolated nephronophthisis, Senior-Loken, Bardet-Biedl and Meckel syndromes[6,7].

Joubert syndrome (JS) is an autosomal recessive disorder presenting with psychomotor delay, hypotonia, ataxia, oculomotor apraxia and breathing abnormalities in the neonatal period[1]. Neuroradiologically, JS is characterized by a peculiar malformation of the midbrain-hindbrain junction known as the “molar tooth sign” (MTS), consisting of cerebellar vermis hypo/aplasia, thick and mal-oriented superior cerebellar peduncles and abnormally deep interpeduncular fossa[2]. The MTS has subsequently been reported in a group of syndromes termed “Joubert Syndrome Related Disorders” (JSRDs), displaying the neurological features of JS associated with involvement of other organs such as the eye and kidney (mainly retinal dystrophy and nephronophthisis). Additional clinical features include optic coloboma, polydactyly, liver fibrosis and other central nervous system malformations[3-4]. At least eight distinct syndromes sharing the MTS have been described so far. However, their nosologic delineation is still problematic due to the wide phenotypic variability both within and among families[5]. Genetic heterogeneity mirrors clinical heterogeneity of JSRDs, with two genes (*AHI1*/JBTS3 and *NPHP1*/JBTS4) and two additional genetic loci (JBTS1 and JBTS2) identified so far[8-13].

Mutations in the *AHI1* gene (chromosome 6q23, MIM[*608894]) account for about 10% of patients with the MTS and lead to a prevalent phenotype of JS plus retinal abnormalities, with the kidneys usually spared[14-16]. Homozygous deletions of *NPHP1* (chromosome 2q13, MIM[*607100]), which represent the most frequent cause of juvenile isolated nephronophthisis, have been described only in four JSRD patients with invariable renal involvement and occasional retinopathy[10,17]. To date, four families with pure cerebellar phenotype are linked to JBTS1 (chromosome 9q34, MIM[%213300]) while linkage to JBTS2 (chromosome 11p12-q13, MIM[%608091]) has been detected in six families characterized by multiorgan involvement and

striking phenotypic variability[18]. In our series, eighteen consanguineous JSRD families did not show linkage to any of the known loci, supporting further genetic heterogeneity. In the largest family (COR27), a simulation study performed with the program SLINK revealed a maximum expected LOD score of 3.60, indicating that this family was informative to detect linkage. A 10-cM resolution genome-wide screen identified a marker on chromosome 12q (D12S1064) that generated a LOD score of 3.46 in family COR27 and positive LOD scores in additional seven smaller families. The region surrounding this marker was saturated with densely spaced microsatellite markers and haplotypes were constructed. A combination of negative LOD scores and the presence of heterozygous genotypes in affected individuals allowed exclusion of linkage in two small families. Conversely, all affected individuals in the remaining six families shared a 2.7 cM region of homozygosity by descent between markers D12S1670 and D12S351, identifying a novel locus which we termed JBTS5 (**Fig. 1**). Pooled LOD scores for the six pedigrees resulted in a maximum cumulated two point LOD score of 8.54 for marker D12S1064 at recombination fraction = 0 (**Supplementary Table 1**). The JBTS5 region spans 8.4 Mb on the physical map of chromosome 12 and contains 21 genes (**Fig. 2a**). The *CEP290* gene, encoding a putative 2480 aa centrosomal protein, was selected as a good candidate because of the key role played by centrosomal and ciliary proteins in several disorders showing overlapping features with JSRDs, such as cystic kidney diseases, Bardet-Biedl and Meckel syndromes[6,7] (**Fig. 2b**). We identified independent homozygous nucleotide changes in *CEP290* in five of the six linked families. Three of these (4732G>T, 5668G>T and 5824C>T) were nonsense mutations resulting in premature truncation of the protein (E1578X, G1890X and Q1942X), and were detected in families from Italy (COR27), Turkey (COR51) and Palestine (MTI133). In family MK05 from Turkey,

we identified a 1 bp deletion in exon 28 (3176delT) resulting in a frameshift and generation of a premature stop codon (I1059fsX1064). The fifth mutation (21G>T), identified in Pakistani family COR22, resulted in a nonconservative W7C substitution that affected a highly conserved residue of the protein (**Fig. 2c**).

All mutations segregated with the disease and were not detected in 300 control chromosomes of Italian and Asian origin. In the remaining family consistent for linkage to JBTS5 (MK20), no coding mutations have been identified to date. Either this family harbors mutations in non-coding regions of *CEP290* or, alternatively, the disease is due to mutations in a distinct, as yet unidentified, gene.

The phenotype associated with *CEP290* mutations is mainly characterized by the neurological features of JS associated with severe retinal and renal involvement. However the clinical spectrum is broad, including incomplete phenotypes such as cerebello-retinal and cerebello-renal syndromes. Additional features are rare, with one patient with cleft palate and another one with possible liver involvement (**Table 1** and **Fig. 3**). The full-blown JBTS5 phenotype overlaps with Senior-Loken syndrome (SLS), characterized by retinitis pigmentosa plus juvenile nephronophthisis and occasionally associated with neurological involvement and the MTS[4,5]. Mutations in most nephronophthisis-related genes, encoding ciliary proteins, have been shown to cause SLS, but neurological and neuroradiological features typical of JS were never reported in these patients[19-22].

We tested the temporal and regional expression of *Cep290* using both RT-PCR and *in situ* hybridization in mouse brain. A full-length murine *Cep290* was assembled from three partially-overlapping cDNA contigs from the human genome browser. The construct encodes a predicted protein that is 89% identical to the full-length human protein on a region syntenic with the human chromosome 12 interval. Northern blot

analysis of whole mouse embryo showed roughly equal expression at embryonic day (E) 7-17 (**Fig. 4a**). We found approximately equal expression levels of the *Cep290* mRNA in various regions from mouse brain across developmental timepoints using RT-PCR (embryonic day 7 through postnatal day 17), suggesting a possible role for this protein in embryogenesis of several brain structures (data not shown). *Cep290* was expressed in multiple organs tested during early postnatal development (P0), with two major transcripts present on Northern blot analysis. Bands of approximately 4.6 and 7.9 kb were detected in roughly equal relative ratios, with the highest levels of expression in the hindbrain, and lower levels in other organs (**Fig. 4b**). The 4.6 kb transcript likely corresponds to cDNA clone AK172940, however no 5' stop codon was detected in this clone. The 7.9 kb transcript corresponds to the full length human and mouse *Cep290* predicted mRNAs. *In situ* hybridization analysis of the cerebellum using a ubiquitous cDNA fragment showed the strongest expression in dividing cell populations of the external granule layer (EGL) during development, suggesting a possible role for *Cep290* in cell division. The gene was also expressed in the internal granule layer cell population (which derive from the EGL through cell migration) in both development and adulthood (**Fig. 4c**). Regions of the telencephalon containing dividing cells also expressed relatively higher levels of *Cep290* (data not shown).

Intracellular localization of mouse CEP290 fused to EGFP was examined in both non-ciliated and ciliated cells. A plasmid encoding the constitutive centrosomal protein Centrin 2 fused to DSRedII (CETN2-RFP), which labels the pair of centrioles, was used to stably transfect 293T human non-ciliated kidney cells. These cells were chosen due to the kidney phenotype observed in our patients. GFP-CEP290 localized to the region surrounding the centrioles (i.e. the pericentriolar matrix) in all

transfected cells (**Fig. 5a**), consistent with the putative centrosomal localization. To test for ciliary localization, we next utilized murine kidney intramedullary collecting duct (IMCD-3) kidney cells that are able to form cilia when grown at confluence. GFP-CEP290 was found to localize to the base of the cilia, as defined by staining for the pericentriolar matrix protein pericentrin and the stabilized microtubule marker acetylated tubulin (**Fig. 5b-c**). A plasmid encoding GFP-CEP290 with the W7C mutation showed localization that was not significantly different from wildtype GFP-CEP290 (data not shown).

The *CEP290* product encodes a large protein with a nearly uninterrupted series of coiled-coil domains. The protein has been first identified as 3H11Ag, a tumour-associated antigen defined by the monoclonal antibody 3H11 that specifically recognizes cancer cells in various neoplastic tissues. The cDNA encoding the protein was subsequently cloned from a gastric cancer cell line and the gene mapped to chromosome 12q[23]. Although the protein function was unknown, Northern blot and RT-PCR experiments showed that 3H11Ag mRNA was extensively distributed in embryonic tissue and in different cancerous tissues, but not in corresponding adult tissues, thus suggesting a role for the underlying protein in embryonic development[23]. Subsequently, 3H11Ag was identified as a centrosomal protein through a mass-spectrometry based proteomic approach, and named *CEP290*[24]. Centrosomes are the major microtubule-organizing centers of animal cells. They are involved in the control of ciliary activity and in regulation of cell shape, polarity, motility and cell division through effects on the mitotic spindle[25,26].

An increasing number of disorders associated with cystic kidney disease have been linked to mutations in proteins expressed in cilia or centrosomes[7]. These proteins share multiple coiled-coil, SH3 and WD40 modular protein-protein interaction

domains. Such proteins may form multimeric complexes in centrosomes and cilia of different tissues, including renal epithelial cells, retinal photoreceptors, cholangiocytes of the bile duct and neuronal axons[6]. Interestingly, the *AHI1* gene product also contains several interaction domains, although its subcellular localization to cilia or centrosomal structures has not been tested[8,9]. These findings provide a unifying frame to understand the pathogenetic mechanism of both isolated renal cystic disorders and distinct pleiotropic syndromes characterized by multiorgan involvement, including JSRDs. Ciliary and centrosomal proteins may interact to respond to extracellular signaling or modulatory cues that are key in maintenance of kidney and retinal homeostasis, and in neuronal development[26,27]. In particular, defective intraciliary and axonal transport could cause impaired axonal outgrowth possibly responsible for the malformations of the cerebellum and brainstem observed in JSRDs. The identification of *CEP290* mutations in patients without renal involvement broadens the phenotypic spectrum associated with disorders of ciliary and centrosomal proteins, and may facilitate the identification of other JSRD genes.

Methods

Patients and families. Eighteen consanguineous families from Europe, the Middle East, Asia and North America were selected on the basis of the following criteria: 1) at least one individual with a neuroradiologically proven MTS associated with any JSRD phenotype; 2) exclusion of linkage to known JBTS loci (JBTS1 to 4). Whenever possible, patients underwent a full diagnostic protocol as previously reported[15]. Parental written informed consent was obtained from all families and the study was approved by the Ethics Committees of UCSD (La Jolla) and CSS-Mendel Institute (Rome).

Genome-wide screen and fine mapping of the JBTS5 locus. The genome-wide

screen was performed in 75 individuals including 26 patients and 49 unaffected first degree relatives, by genotyping 402 microsatellite markers (Marshfield Screening Set 13) with an average inter-marker distance of 10cM. Two-point LOD scores were generated using the FASTLINK version of the MLINK program, assuming equal male-female recombination rate, autosomal recessive inheritance, a gene frequency of 0.001 with complete penetrance and equal allele frequencies for each marker[28]. To saturate the 8.4 Mb region surrounding marker D12S1064, additional markers were selected from the May 2004 UCSC draft of the Human Genome. As no informative markers were available in a 5.2 Mb interval within the locus, we generated two novel microsatellite markers using the Tandem Repeat Finder software, as previously reported[13]. Details of these new markers are in **Supplementary Table 2**. Genomic DNA was PCR-amplified using fluorescent primers. Amplified fragments were run on an ABI Prism 3100 DNA sequencer and analyzed with GeneScan and Genotyper software (Applied Biosystems). Haplotypes were manually constructed, and phase was assigned based on the minimum number of recombinants.

Mutation analysis. PCR primers to amplify *CEP290* 53 coding exons and exon-intron boundaries were manually designed on the chromosome 12 draft of the human genome (**Supplementary Table 3**). Sequencing analysis was carried out using the dideoxy chain termination method (BigDye 3.0) on an ABI 3100 DNA automated sequencer according to standard procedures and the manufacturer's recommendations (Applied Biosystems). Sequences of affected individuals were analyzed and compared to those of controls by using the SeqMan software (DNASTAR Inc.). Identified mutations were confirmed at least twice by bidirectional sequencing.

Gene expression analysis with quantitative RT-PCR. We purified total RNA from

whole brain, cerebellum and cortex of mice (E14, E16, E18, P5, P10 and adult) using a standard Trizol method (Invitrogen). cDNA was reverse-transcribed from total RNA (5 µg) using SuperScript™ III First-Strand Synthesis System (Invitrogen) with oligo(dT) primers. We PCR-amplified a ubiquitous fragment at 3' of *Cep290* ORF (primer forward: 5'-GAGACCAAGATGAAAGAGCTTGA-3'; reverse: 5'-GCTTTTTAACTTCCTCCTTCG-3') and GAPDH as an internal control. Each reaction was run in triplicate, and a negative control without cDNA template was run with each assay. Band intensities were quantified by ImageQuant v1.1 (Molecular Dynamics) and band intensities for *Cep290* were standardized with *Gapdh* internal controls[8].

Mouse *in situ* hybridization. *In situ* hybridization on frozen mouse brain sections was performed using a non-radioactively digoxigenin-labeled cDNA probe. The *Cep290* probe was amplified from mouse embryonic day 18 (E18) with primers specific to the three longest *Cep290* mRNA transcripts (forward 5'-GAATGCTCTAGCCCAAGCAC-3'; reverse 5'-GTGGGCTTCTCCTTCCTTCT-3'). The 739bp probe was cloned into pCR-Blunt II-TOPO vector containing SP6 and T7 promoter priming sites. Antisense cDNA probe transcription was driven from the T7 promoter and transcription of the sense cDNA probe driven from the SP6 promoter. Mouse brain sections from embryonic through adult timepoints were fixed, and then hybridized using the digoxigenin-labeled cDNA probes overnight at 65°C. Sections were washed, treated with RNAase and washed again before being treated with anti-dixoxgenin coupled to alkaline phosphatase (Roche). After a further wash in 5M NaCl, 1M Tris base, 1M Tris-Hcl, 2M MgCl2 and 10% Tween-20, the digoxigenin-labeled cDNA probe was detected using NBT and BCIP and sections were stained overnight at room temperature.

Northern-blot analysis. We used the same *Cep290* mouse genome sequence to

generate the *in situ* probe for the Northern Blot analysis. The probe was labelled with [α-32P]dCTP using the Prime-It II Random Primer Labeling Kit (Stratagene). A Clontech polyA-selected commercial blot was used to interrogate whole body expression. For specific organ analysis, total RNA was isolated from post-natal day 0 multiple mouse tissues using Trizol and tested for *Cep290* expression. After probe hybridization, the blots were developed according to the ExpressHyb Hybridization protocol (Clontech).

Fluorescence microscopy. The full length mouse *Cep290* (Accession XM_618806) was amplified with forward 5'-ATGCCACCTAATATAAAGTGGAAAGA-3' and reverse 5'-ATAACACAGAGACTGCTTGATTTCC–3' primers using Platinum® High Fidelity *Taq* DNA Polymerase (Invitrogen) and cloned into pCR®-XL-TOPO (Invitrogen) in reverse orientation. It was then sub-cloned into *Xho*I and *Bam*HI sites of mammalian expression vector pEGFP-C3 (Clontech). The patient missense mutation was introduced by site directed mutagenesis. The open reading frame of each clone was fully sequenced before use. 293T cells were transfected with RFP-CETN2 and stable cell lines were established. These were subsequently transfected with GFP-CEP290 and imaged 2 days later. IMCD-3 (ATTC) cells were transfected at 80% confluence, allowed to grow to confluence and develop cilia, then fixed and stained with antibodies to acetylated α-tubulin (Zymed), pericentrin (PRB-432, Covance), and centrin 2 (hCetn2.4 ascites, gift from J. Salisbury, Mayo). Images were captured on a DeltaVision deconvolution microscope and processed with Softworks software.

URLs. The mouse and human genome databases from the University of California at Santa Cruz and NCBI are available at http://genome.ucsc.edu/ and http://www.ncbi.nlm.nih.gov/ respectively.

Accession numbers. GenBank: human *CEP290* mRNA, NM_025114; the full-length mouse mRNA, XM_618806 has been removed from the database and is constituted by the following cDNAs: AK172940, BI733169, CO043781, BE571692, and CB181153 with a small gap in the 5' part of the ORF. GenBank protein: human full-length CEP290 protein isoform, NP_079390.

Acknowledgements

We thank the Marshfield Clinic Research Foundation and NHBLI for genotyping support. We also thank Dr Carla Uggetti (UO Pediatric Neuroradiology, IRCCS "C. Mondino Foundation", University of Pavia) for her valuable contribution in reviewing MRIs of selected patients. We received help with imaging from Brendan Brinkman and the UCSD Neuroscience Microscopy Core and help with *in situ* hybridization from Wendy Books in the Hamilton lab. This work was supported by grants from the U.S. National Institute of Neurological Disease and Stroke, the Italian Ministry of Health (Ricerca Corrente 2006; Ricerca Finalizzata 2005 Progetto Malattie Rare Conv. 526/A36), the Fondazione Pierfranco e Luisa Mariani ONLUS, the March of Dimes, the Simons Foundation and the Burroughs Wellcome Fund Award in Translational Research.

References

1. Joubert, M., Eisenring, J.J., Robb, J.P. & Andermann, F. Familial agenesis of the cerebellar vermis. A syndrome of episodic hyperpnea, abnormal eye movements, ataxia, and retardation. *Neurology* **19**, 813–825 (1969).

2. Maria, B.L. *et al*. "Joubert syndrome" revisited: key ocular motor signs with magnetic resonance imaging correlation. *J. Child Neurol.* **12**, 423–430 (1997).

3. Saraiva, J.M. & Baraitser, M. Joubert syndrome: a review. *Am. J. Med. Genet.* **43**, 726–731 (1992).

4. Satran, D., Pierpont, M.E. & Dobyns, W.B. Cerebello-oculo-renal syndromes including Arima, Senior-Loken and COACH syndromes: more than just variants of Joubert syndrome. *Am. J. Med. Genet.* **86**, 459–469 (1999).

5. Gleeson, J.G. *et al*. Molar tooth sign of the midbrain-hindbrain junction: occurrence in multiple distinct syndromes. *Am. J. Med. Genet.* **125A**,125–134 (2004).

6. Hildebrandt, F. & Otto, E. Cilia and centrosomes: a unifying pathogenic concept for cystic kidney disease? *Nat. Rev. Genet.* **6**, 928-940 (2005).

7. Katsanis, N. Ciliary proteins and exencephaly. *Nat. Genet.* **38**, 135-136 (2006).

8. Dixon-Salazar, T. *et al*. Mutations in the AHI1 Gene, Encoding Jouberin, Cause Joubert Syndrome with Cortical Polymicrogyria. *Am. J. Hum. Genet.* **75**, 979–987 (2004).

9. Ferland, R.J. *et al*. Abnormal cerebellar development and axonal decussation due to mutations in AHI1 in Joubert syndrome. *Nat. Genet.* **36**, 1008–1013 (2004).

10. Parisi, M.A. *et al*. The NPHP1 gene deletion associated with juvenile nephronophthisis is present in a subset of individuals with Joubert syndrome. *Am. J. Hum. Genet.* **75**, 82–91 (2004).

11. Saar, K. *et al*. Homozygosity mapping in families with Joubert syndrome identifies a locus on chromosome 9q34.3 and evidence for genetic heterogeneity. *Am. J. Hum. Genet.* **65**, 1666–1671 (1999).

12. Keeler, L.C. *et al*. Linkage analysis in families with Joubert syndrome plus oculo-renal involvement identifies the CORS2 locus on chromosome 11p12-q13.3. *Am. J. Hum. Genet.* **73**, 656–662 (2003).

13. Valente, E.M. *et al*. Description, nomenclature, and mapping of a novel cerebello-renal syndrome with the molar tooth malformation. *Am. J. Hum. Genet.* **73**, 663–670 (2003).

14. Parisi, M.A. *et al*. AHI1 mutations cause both retinal dystrophy and renal cystic disease in Joubert syndrome. *J. Med. Genet*. 2005 Sep 9 [advance online publication].

15. Valente, E.M. *et al*. AHI1 gene mutations cause specific forms of Joubert syndrome-related disorders. *Ann. Neurol.* **59**, 527-534 (2006)

16. Utsch, B. *et al*. Identification of the first AHI1 gene mutations in nephronophthisis-associated Joubert syndrome. *Pediatr. Nephrol.* 2005 Oct 21 [advance online publication].

17. Castori, M. *et al*. NPHP1 gene deletion is a rare cause of Joubert Syndrome Related Disorders. *J. Med. Genet.* **42**, e9 (2005).

18. Valente, E.M. *et al*. Distinguishing the four genetic causes of Joubert syndrome-related disorders. *Ann. Neurol.* **57**, 513–519 (2005).

19. Caridi, G. *et al*. Clinical and molecular heterogeneity of juvenile nephronophthisis in Italy: insights from molecular screening. *Am. J. Kidney Dis.* **35**, 44-51 (2000).

20. Olbrich, H. *et al*. Mutations in a novel gene, NPHP3, cause adolescent nephronophthisis, tapeto-retinal degeneration and hepatic fibrosis. *Nat. Genet.* **34**, 455-459 (2003).

21. Otto, E. *et al*. A gene mutated in nephronophthisis and retinitis pigmentosa encodes a novel protein, nephroretinin, conserved in evolution. *Am. J. Hum. Genet*. **71**, 1161-1167 (2002).

22. Otto, E.A. *et al*. Nephrocystin-5, a ciliary IQ domain protein, is mutated in Senior-Loken syndrome and interacts with RPGR and calmodulin. *Nat. Genet.* **37**, 282-288 (2005).

23. Chen, D. & Shou, C. Molecular cloning of a tumor-associated antigen recognized by monoclonal antibody 3H11. *Biochem. Biophys. Res. Commun.* **281**, 1356-1357 (2001).

24. Andersen, J.S., Wilkinson, C.J., Mayor, T., Mortensen, P., Nigg, E.A. & Mann, M. Proteomic characterization of the human centrosome by protein correlation profiling. *Nature* **426**, 570-574 (2003).

25. Doxsey, S. Re-evaluating centrosome function. *Nature Rev. Mol. Cell Biol.* **2**, 688-698 (2001).

26. Badano, J.L., Teslovich, T.M. & Katsanis, N. The centrosome in human genetic diseases. *Nature Rev. Genet.* **6**, 194-205 (2005).

27. Louie, C.M. & Gleeson, J.G. Genetic basis of Joubert syndrome and related disorders of cerebellar development. *Hum. Mol. Genet.* **14 Spec No 2**, R235-242 (2005).

28. Cottingham Jr, R.W., Idury, R.M. & Schaffer, A.A. Faster sequential genetic linkage computations. *Am. J. Hum. Genet.* **53**, 252-263 (1993).

Appendix

Other members of the International JSRD Study Group are as follows:

Richard Leventer (Parkville, Australia); Padraic Grattan-Smith (Sydney, Australia); Andreas Janecke (Innsbruck, Austria); Marc D'Hooghe (Brugge, Belgium); Rudy Van Coster (Ghent, Belgium); Karin Dias, Carla Moco, Ana Moreira (Porto Alegre, Brazil); Chong Ae Kim (Sao Paulo, Brazil); Gustavo Maegawa (Toronto, Canada); Ghada M.H. Abdel-Salam, Alice Abdel-Aleem, Maha S. Zaki (Cairo, Egypt); Itxaso Marti, Susana Quijano-Roy (Garches, France); Pascale de Lonlay, Stéphane Romano, Alain Verloes (Paris, France); Renaud Touraine (St. Etienne, France); Michel Koenig, Clotilde Lagier-Tourenne, Jean Messer (Strasbourg, France); Heike Philippi (Mainz, Germany); Sofia Kitsiou Tzeli (Athens, Greece); Saevar Halldorsson (Reykjavik, Iceland); Shubha R. Phadke (Lucknow, India); Bernard Stuart (Dublin, Ireland); Alex Magee (Belfast, Northern Ireland); Dorit Lev (Holon, Israel); Bruria Ben-Zeev (Ramat-Gan, Israel); Rita Fischetto, Mattia Gentile (Bari, Italy); Silvia Battaglia, Lucio Giordano (Brescia, Italy); Martino Ruggieri (Catania, Italy); Stefania Bigoni, Alessandra Ferlini (Ferrara, Italy); Maria Alice Donati, Elena Procopio (Florence, Italy); Gianluca Caridi, Francesca Faravelli, Gianmarco Ghiggeri (Genoa, Italy); Silvana Briuglia, Carmelo D. Salpietro, Gaetano Tortorella (Messina, Italy); Stefano D'Arrigo, Chiara Pantaleoni, Daria Riva, Graziella Uziel (Milan, Italy); Anna Maria Laverda, Alberto Permunian (Padova, Italy); Stefania Bova (Pavia, Italy); Roberta Battini (Pisa, Italy); Maria Roberta Cilio, Marilù Di Sabato, Francesco Emma, Vincenzo Leuzzi, Pasquale Parisi (Rome, Italy); Alessandro Simonati (Verona, Italy); Mirjam M. de Jong (Groningen, The Netherlands); Matloob Azam (Islamabad, Pakistan); Berta Rodriguez (La Coruna, Spain); Ignacio Pascual-Castroviejo (Madrid, Spain); Hulya Kayserili (Istanbul, Turkey); Lihadh Al Gazali, Laszlo Sztriha (Al Ain,

UAE); David Nicholl (Birmingham, UK); C. Geoffrey Woods (Cambridge, UK); Raoul Hennekam (Oxford, UK); Saunder Bernes (Mesa, Arizona, US); Henry Sanchez (Fremont, California, US); Aldon E. Clark (Laguna Niguel, California, US); Elysa DeMarco, Clement Donahue, Elliot Sherr (San Francisco, California, US); Jin Hahn, Terence D. Sanger (Stanford California, US); Tomas E. Gallager (Manoa, Hawaii, US); William B. Dobyns (Chicago, Illinois, US); Cynthia Daugherty (Bangor, Maine, US); Kalpathy S. Krishnamoorthy, Dean Sarco, Christopher A. Walsh (Boston, Massachusetts, US); Trudy McKanna (Grand Rapids, Michigan, US); Joanne Milisa (Albuquerque, New Mexico, US); Wendy K. Chung, Darryl C. De Vivo, Hillary Raynes, Romaine Schubert (New York, New York, US); Alison Seward (Columbus, Ohio, US); David G. Brooks (Philadephia, Pennsylvania, US); Amy Goldstein (Pittsburg, Pennsylvania, US); James Caldwell, Eco Finsecke (Tulsa, Oklahoma, US); Kenton Holden (Mt. Pleasant, South Carolina, US); Robert P.Cruse (Houston, Texas, US); Kathryn J. Swoboda, Dave Viskochil (Salt Lake City, Utah, US).

Figure legends

Figure 1

Pedigrees of JBTS5 linked families and haplotypes spanning the linked region. All affected individuals shared a 2.7 cM region of homozygosity between markers D12S1670 and D12S351(dashed lines). In each family, a black bar denotes markers of the disease haplotype which are homozygous by descent in affected members, while the remaining markers of the same haplotype are represented as a white bar. Thin vertical lines interrupting the bars denote recombination events to the non-disease parental chromosome. Horizontal lines above symbols denote individuals who were clinically examined. Deceased individuals are marked by a diagonal line across symbols.

Figure 2

Identification of the *CEP290* gene within the JBTS5 region. a) Genetic map of the JBTS5 locus and detailed physical map showing the location of genetic flanking markers and genes of the region. Arrows indicate the transcriptional direction of each gene. *CEP290* is highlighted in blue. b) The 54 exons and the exon-intron structure of the *CEP290* gene are represented as vertical bars. The start (ATG) and stop (TAA) codons are indicated. c) Electropherograms of mutations found in five probands (upper panels) and healthy controls (lower panels).

Figure 3

Magnetic Resonance Imaging of probands with *CEP290* mutations. a,c,e,g,i (upper panel) and j (lower panel): axial sections at the pontine or ponto-mesencephalic level demonstrating the molar tooth sign (arrows); b,d,f,h (lower panel): paramedian

sagittal sections, showing the thickening and malorientation of superior cerebellar peduncles (arrows) and cerebellar vermis hypoplasia (arrowheads). For family COR51, sagittal sections were not available but axial sections of both affected siblings are presented (i: patient II:1 and j: patient II:2).

Figure 4

Expression pattern of *Cep290* in mouse. a) Northern blot from whole mouse embryo at specific embryonic (E) days show a 4.6 kb band. b) mouse tissues at postnatal day 0 showing bands at approximately 7.9 and 4.6 kb, with relatively higher expression in hindbrain compared with other regions. Bottom shows the same blots probed for G3PDH for loading control. c) *In situ* hybridization from embryonic (E) or postnatal (P) mouse cerebellum. Expression was noted in the external (arrowhead) and internal (arrow) granule layer (EGL and IGL) in the midline prior to foliation. Asterisk is choroid. At older ages during and after foliation, expression persists in this cell population. Scale bar = 200 μm.

Figure 5

Cep290 localizes to the centrosome and cilia in kidney cells. a) Human 293T cells. The arrow shows co-distribution of GFP-CEP290 (green) with the constitutive centrosomal marker RFP-CETN2. b-c) Intramedullary collecting duct (IMCD-3) murine kidney ciliated cells. Arrows show co-localization of GFP-CEP290 (green) with the pericentriolar matrix protein pericentrin (red, panel b), and with the base of the cilia (panel c). Arrowhead in panel (c) indicates the cilium marked by acetylated tubulin staining (red). In all panels, nuclei are stained blue with Hoechst. Scale bar = 5 μm.

Table 1

Clinical findings of patients with *CEP290* homozygous mutations

Family	COR27			COR51		MTI-133		COR22	MK05
Country of origin	Sardinia (Italy)			Turkey		Palestine		Pakistan	Turkey
Nucleotide change (exon)	4732G>T (36)			5668G>T (41)		5824C>T (42)		21G>T (2)	3176delT (28)
Protein mutation:	E1578X			G1890X		Q1942X		W7C	I1059fsX1064
patient (sex)	V:1 (F)	V:2 (F)	V:4 (F)	II:1 (M)	II:2 (M)	II:1 (M)	II:2 (M)	II:1 (M)	II:2 (F)
Age at examination	15 yrs	3 yrs	10 yrs	17 yrs	15 yrs	dead 4mo	dead 7mo	3 yrs	3 yrs
Neurological signs:									
- hypotonia/ataxia	+	+	+	+	+	+	+	+	+
- psychomotor delay	+	+	+	+	+	+	+	+	+
- mental retardation	+	+	+	+	+	n.a.	n.a.	+	+
- OMA	+	+	+	+	+	+	+	+	?
- breathing abnormalities	+	–	–	+	–	+	+	–	+
- other abnormalities	ny	ny	ny, ptosis	–	–	–	–	ny	ny
Ocular signs:									
- retinopathy	CB	CB	CB	RP, vr	RP, vr	–	–	CB	RP, vr
- other abnormalities	–	–	micropht LE	–	drusen in LE	–	–	–	–
Renal signs:									
- NPH/UCD	–	n.a.	–	+	+	n.a.	n.a.	n.a.	n.a.
- kidney ultrasound	normal	normal	normal	n.a.	CC	CC	normal	CC, reduced CMD	CC
Other organs:									
- Liver abnormalities	–	–	–	–	–	–	–	ELE, abnormal US	?
- Other abnormalities	aggressive beh	–	–	–	–	–	cleft palate	autistic beh	–
MRI features:									
- MTS	+	+	+	+	+	+	+	+	+
- other abnormalities	–	–	–	–	–	–	–	–	–

Legend: – Absent; + Present; beh-behavior; CB-congenital blindness; CC-cortical cysts; CMD-cortico-medullar differentiation; ELE-elevated liver enzymes; Hyd-hydrocephalus; LE-left eye; micropht-microphtalmus; mo-months; MTS-molar tooth sign; n.a.-not applicable; NPH/UCD-Nephronophthisis / Urine Concentration Defect; ny-nystagmus; OMA-Oculomotor Apraxia; RP-retinitis pigmentosa; US-ultrasound; vr-visus reduction, yrs-years; ?-unknown

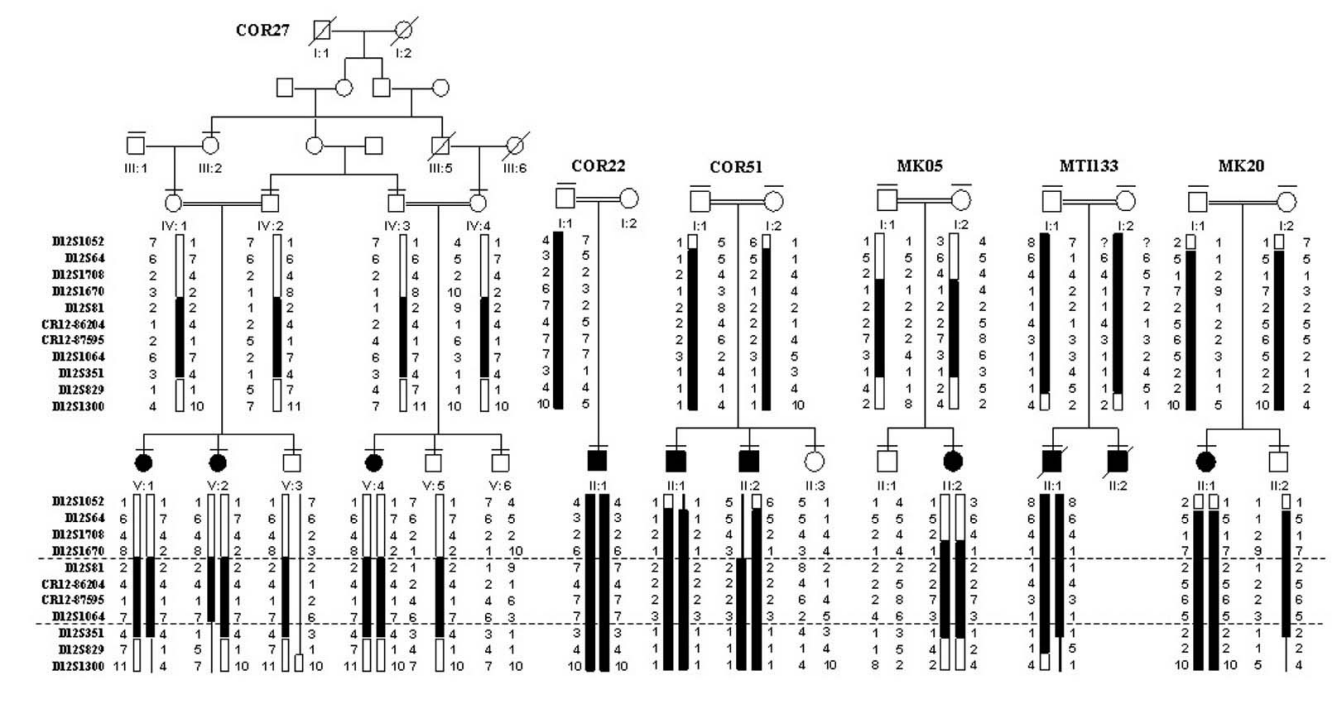
COR27
I:1
I:2
III:1
III:2
III:5
III:6
IV:1
IV:2
IV:3
IV:4
D12S1052
D12S64
D12S1708
D12S1670
D12S81
CR12-86204
CR12-87595
D12S1064
D12S351
D12S829
D12S1300
V:1
V:2
V:3
V:4
V:5
V:6
COR22
I:1
I:2
II:1
COR51
I:1
I:2
II:1
II:2
II:3
MK05
I:1
I:2
II:1
II:2
MTI133
I:1
I:2
II:1
II:2
MK20
I:1
I:2
II:1
II:2

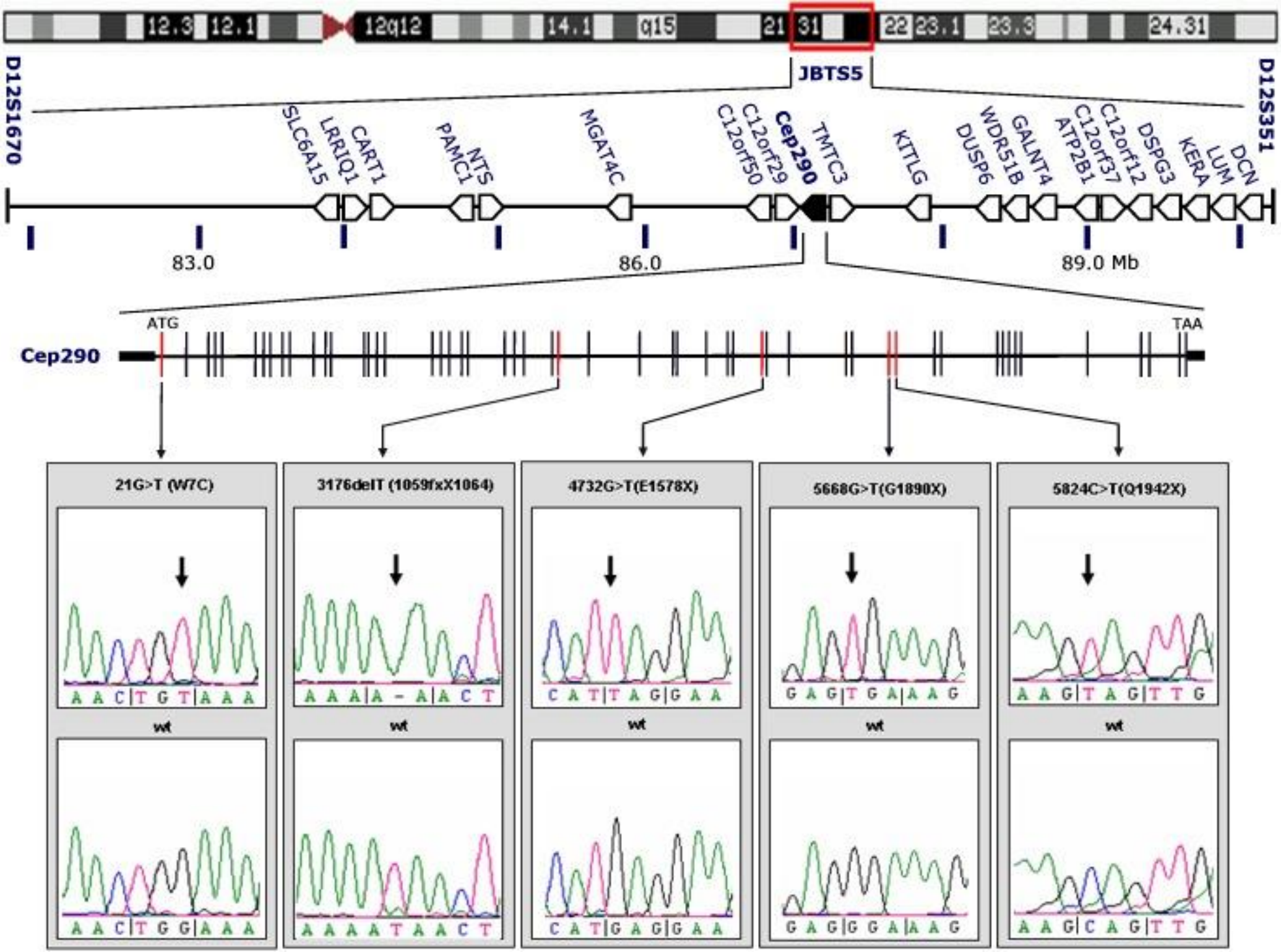
12.3
12.1
12q12
14.1
q15
21
31
22
23.1
23.3
24.31
D12S1670
JBTS5
D12S351
SLC6A15
LRRIQ1
CART1
PAMC1
NTS
MGAT4C
C12orf50
C12orf29
Cep290
TMTC3
KITLG
DUSP6
WDR51B
GALNT4
ATP2B1
C12orf37
C12orf12
DSPG3
KERA
LUM
DCN
83.0
86.0
89.0 Mb
ATG
TAA
Cep290
21G>T (W7C)
3176delT (1059fxX1064)
4732G>T(E1578X)
5668G>T(G1890X)
5824C>T(Q1942X)
wt
wt
wt
wt
wt

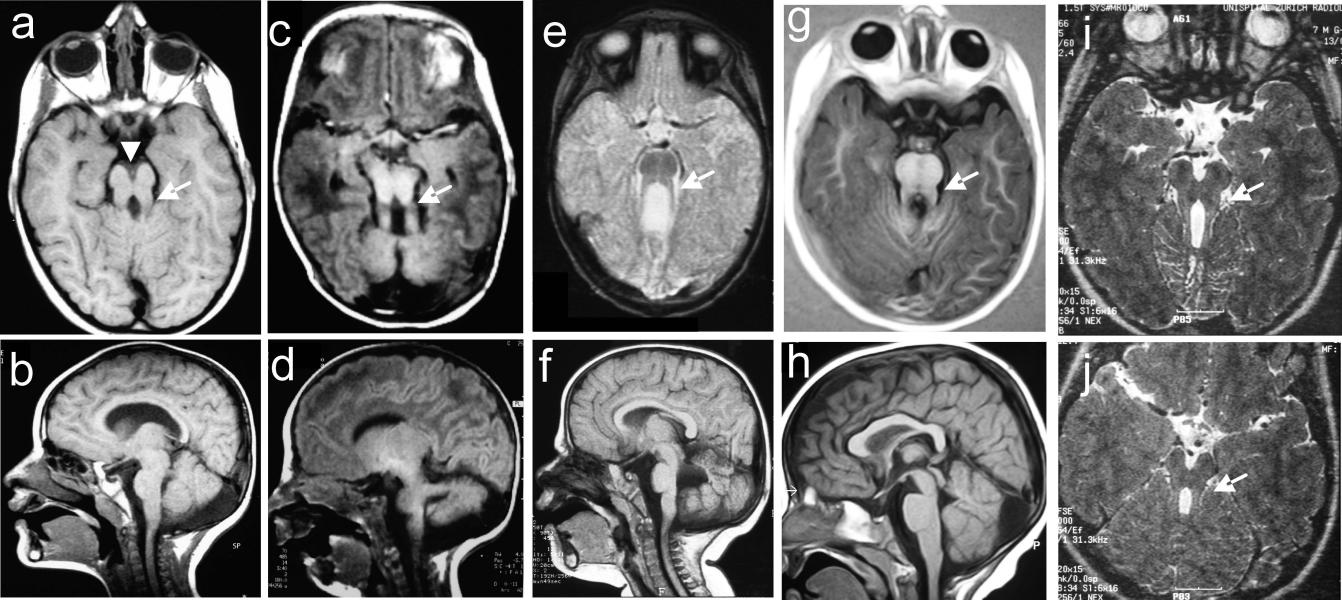
a
c
e
g
i
b
d
f
h
j

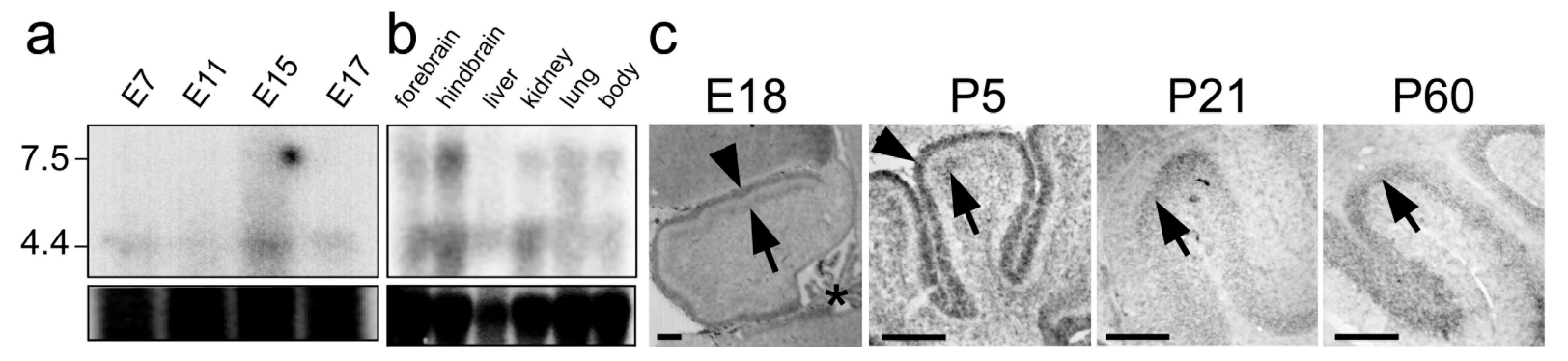
a
E7
E11
E15
E17
7.5
4.4
b
forebrain
hindbrain
liver
kidney
lung
body
c
E18
P5
P21
P60

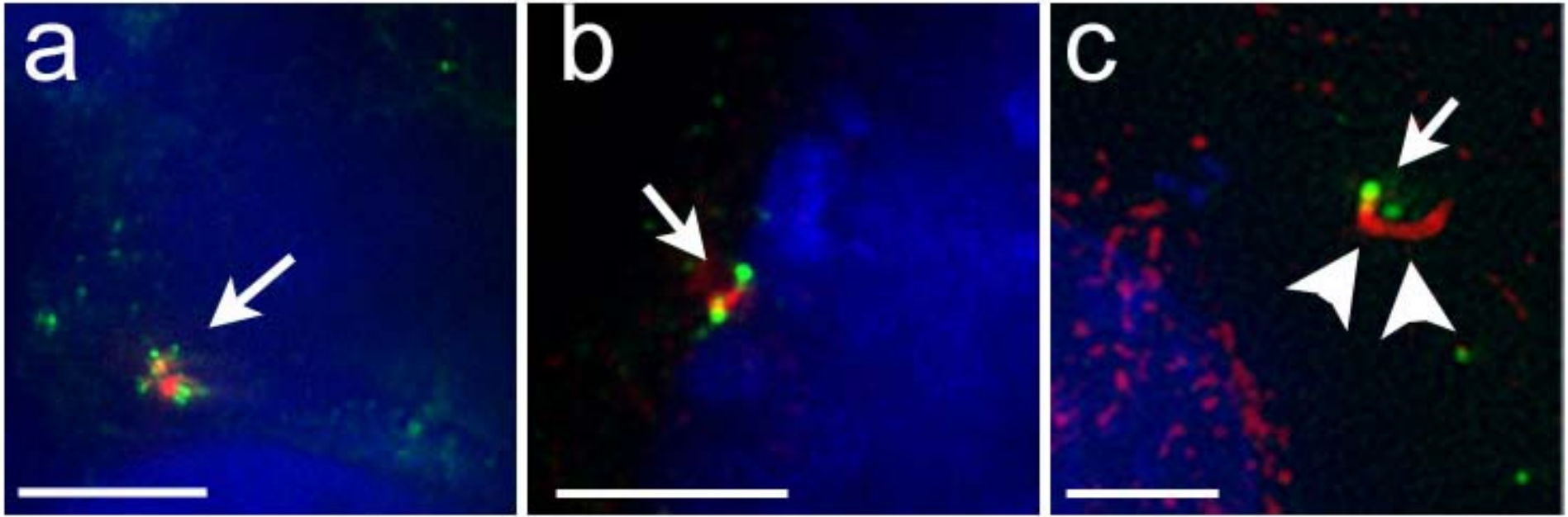
a
b
c